ARTICLES

UV−Vis and FT-IR Study of the Nature and Location of the Active Sites of Partially Exchanged Co−H Zeolites

Tania Montanari,[†] Maria Bevilacqua,[†] Carlo Resini,[†,‡] and Guido Busca*[,†]

Laboratorio di Chimica delle Superfici e Catalisi Industriale, Dipartimento di Ingegneria Chimica e di Processo, Università di Genova, p.le J. F. Kennedy, 1, I-16129 Genova, Italy, and INFM, c/o Dipartimento di Fisica, Università di Genova, Via Dodecaneso, 33, I-16146 Genova, Italy

Received: March 29, 2003; In Final Form: November 20, 2003

A study of the nature and accessibility of internal and external protonic and cationic sites has been carried out on protonic and partially Co-exchanged FER, MFI, and MOR through the use of UV−vis and FT-IR spectroscopy. The ion-exchange procedure was exactly the same for the three zeolites. A sample of Co-exchanged silica−alumina has also been investigated for comparison. UV−vis spectra recorded after outgassing at 773 K provide evidence of the presence of low-coordination Co^{2+} sites in all outgassed Co-containing samples. However, they show that the sites located in the zeolite cavities cannot be distinguished from those located at the open surfaces. FT-IR studies of the adsorption of benzonitrile and *o*-toluonitrile, used as differently hindered weak basic molecules, allowed us to distinguish sites located at the external surfaces or in different cavities. Benzonitrile enters only the main channels of H−MOR and Co−H−MOR, whereas it is not able to enter the mouths of the side pockets. Benzonitrile also enters the channels of H−MFI and Co−H−MFI. *o*-Toluonitrile enters the main channels of H−MOR but does not enter the main channels of Co−H−MOR. Similarly, it slowly enters the channels of H−MFI but does not enter those of Co−H−MFI. So, it provides evidence for the narrowing of the pores of MOR and MFI by Co exchange. Both nitriles do not enter at all the channels of H−FER and Co−H−FER but provide evidence for the location of Co ions at the outer surface. In all cases terminal silanols and Lewis sites are located at the external surfaces, whereas the strongly acidic bridging OHs are exclusively located in the interior of the cavities. In Co−H zeolites, Co^{2+} ions are distributed between internal and external surfaces. The extent of exchange of the internal OHs roughly depends directly on the cavity dimensions, increasing in this sense: FER < MFI < MOR and MOR (side pockets) < MOR (main channels). The data also show that, at least for MFI, cation exchange essentially occurs at the mouth of the channels.

Introduction

Protonic zeolites are widely used as solid acid catalysts for environmentally friendly acid-catalyzed reactions.[1] The active acid sites for adsorption and catalysis on protonic zeolites are associated with bridging Si−(OH)−Al groups which arise from the Al for Si substitution in the framework. As these sites are located in the internal channels, shape selectivity effects may also take place. Catalysis can, however, also occur at the external surface where shape selectivity is not active, thus decreasing the performances of the catalyst.[2,3] Previous studies from our laboratory were devoted to the differentiation of the acid sites located at the external surface and at the internal cavity surfaces of different protonic zeolites. It has been demonstrated that bridging Si−(OH)−Al sites are located exclusively in the cavities, at least in the cases of H−FER,[4,5] H−MFI,[5,6] and H−MOR.[7,8] In multiple pore zeolites, such as H−MOR, the sites located in different cavities can be distinguished.[7,8] At the external surface less acidic terminal silanol groups exist, which retain, however, significant activity.[4−8] Evidence for the location of extraframework material in the interior of the cavities of H−MFI[9] and H−MOR[8] has also been provided.

Co-containing zeolites, such as Co−FER, Co−MFI, and Co−MOR, are active in hydrocarbon dehydrogenation,[10] ammoxidation,[11] and NO reduction with methane in an oxidizing atmosphere,[12−14] so allowing the denitrification (de-NOxing) of waste gases. Co^{2+} ions exchanging the protons of the protonic zeolites are considered to be the active sites.[15] In a number of recent papers the UV−vis spectra of outgassed Co−FER, Co−MFI, and Co−MOR have been studied in detail and assigned to Co^{2+} ions in different locations in the zeolite cavities.[16−19] The possible cooperation between protonic and Co cationic sites in partially exchanged Co zeolites for the CH_4−SCR (selective catalytic reduction) reaction has also been discussed.[13,14,20] The external surface sites' and extraframework material's possible roles in this reaction have not been taken into account.

In the present paper we will investigate the nature and location of the protonic and cationic sites of Co−H−FER, Co−H−MFI, and Co−H−MOR zeolites by UV−vis and IR spectroscopy of

* Corresponding author. E-mail: Guido.Busca@unige.it.
† Dipartimento di Ingegneria Chimica e di Processo.
‡ INFM, c/o Dipartimento di Fisica.

10.1021/jp034814o CCC: $27.50
Published on Web 01/22/2004

TABLE 1: Experimental Composition of the Samples as Determined by Chemical Analysis and Residual Intensity of the O−H-Stretching Band

	Si/Al exptl	Si/Al theoret	Co (wt %) exptl	Co/Al exptl	residual νOH (intensity %) silanol OH	residual νOH (intensity %) bridging OH
Co−H−FER	28.51	27.5	2.21	0.73	70	88
Co−H−MFI	28.31	25.0	1.71	0.55	57	50
Co−H−MOR	10.06	10.0	4.92	0.68	89	33

adsorbed hindered nitriles, with the aim of gaining information also on the external surface of such zeolites. Benzonitrile (BZN) and *o*-toluonitrile (*o*-TN) have been chosen for their steric hindrance related to the size of the cavities of these zeolitic materials.

Experimental Section

Preparation Procedures. NH_4−FER (SiO_2/Al_2O_3 = 55, surface area (S) = 480 $m^2\ g^{-1}$), NH_4−MFI (SiO_2/Al_2O_3 = 50, S = 425 $m^2\ g^{-1}$), and NH_4−MOR (SiO_2/Al_2O_3 = 20, S = 480 $m^2\ g^{-1}$) supplied by Zeolyst were used as starting materials. NH_4−zeolite powders were contacted with a 0.02 M $(CH_3COO)_2Co{\cdot}4H_2O$ aqueous solution (10 g of powder for 1 L of solution) under stirring at a constant temperature of 353 K for 24 h. The resulting slurry was filtered, and the solid was washed three times with doubly distilled water. After centrifugation, the powders were dried at 353 K for 10 h and calcined at 823 K for 4 h.

A similar procedure has been applied to the production of Co−silica−alumina from silica−alumina (13% Al_2O_3, from STREM Chemicals, S = 300 $m^2\ g^{-1}$). The resulting Co loadings are around 10 w/w % for Co−silica−alumina and are reported in Table 1 for Co zeolites.

Characterization Techniques. Diffuse reflectance spectra (DR−UV−vis−NIR) of disks of the pure powders have been recorded by use of a Jasco V-570 spectrometer after dehydration at 773 K for 5 h by outgassing through a conventional gas manipulation−outgassing ramp connected to a quartz cell.

The IR spectra were recorded on a Nicolet Protégé 460 and a Nicolet Magna 750 Fourier transform instrument. The surface characterization has been performed using pressed disks of pure powders (15 mg for a disk of 2 cm diameter), activated by outgassing at 773 K into the IR cell. A conventional manipulation−outgassing ramp connected to the IR cell was used. The adsorption procedure involves contacting the activated sample disks with vapors at room temperature (RT) and a pressure of 15 Torr and outgassing in steps at RT and increasing temperatures. The nitriles used for adsorption were from Aldrich.

Results and Discussion

UV−Vis Spectroscopic Characterization. In Figure 1 the spectra of partially cobalt-exchanged FER, MFI, and MOR recorded after evacuation at 773 K for 5 h are reported. The very high-energy region (above 40 000 cm^{-1}) is unavailable in the spectrum because our vacuum cell causes strong noise there. Absorptions are found in all three cases which can be interpreted as a triplet near 19 000, 17 000, and 15 000 cm^{-1}. No other absorption occurs in the range of 40 000−22 000 cm^{-1}. The spectra we observe are close to those reported and deeply discussed by Kauchy et al. for Co−FER,[16] Dedecek and coworkers for Co−MOR[17] and Co−MFI,[18] and Drozdova et al.[19] for all three Co−H zeolites.

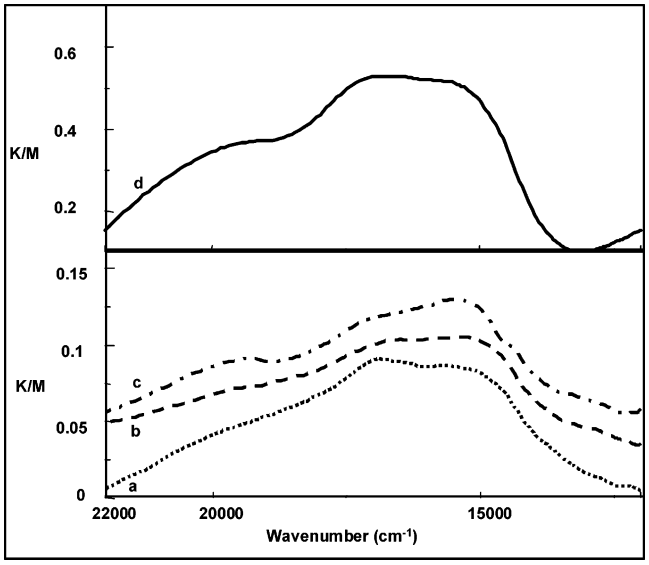

Figure 1. DR−UV−vis spectra of samples outgassed for 5 h at 773 K: spectrum a, Co−H−FER; spectrum b, Co−H−MFI; spectrum c, Co−H−MOR; spectrum d, Co−H−silica−alumina.

These authors, who investigated Co−H−FER and Co−H−MOR samples with much less Co loading than our samples and a Co−H−MFI sample with a similar Co loading but a lower Co/Al atomic ratio, claim that each of these absorptions is the strongest band of a more complex absorption band system. They single out three different Co sites, namely α, β, and γ. These authors observe that the wavelengths of the maxima of the individual spectral bands corresponding to the α-, β-, and γ-Co ions are very similar. This indicates similar coordination of the individual Co ions in MFI, FER, and MOR.

It is suggested that the α-type Co ions are located in the main channel of MOR and FER as well as in the straight channels of the MFI structure, coordinated to framework oxygens of the six-membered rings composed of two five-membered rings. The β-type Co ions would be located in the twisted eight-membered rings of the MOR cavity, in the deformed six-membered rings of the FER cavity, and at the deformed six-membered rings at the intersection of the straight and the sinusoidal channels of the MFI structure. The Co ions at the γ-type would be at the so-called "boat-shaped" site of MOR and in analogous framework local structures found in FER and MFI.[19]

To check the picture given by the above cited authors,[16−19] we further investigated, under the same conditions, the UV spectroscopy of other Co-containing samples, such as Co−silica−aluminas. We find with these samples again a very similar spectrum, with a triplet in the region of 22 000−14 000 cm^{-1} (Figure 1, upper spectrum). So, we conclude that the spectrum of Co sites in an open external surface, such as that of Co−silica−alumina, is indistinguishable from those of Co sites in the zeolite cavities. For this reason, in our opinion the detailed assignments of the absorptions in the region of 22 000−14 000 cm^{-1} to specific sites located at particular positions in the cavities of the three zeolites is quite unreliable. Nevertheless, we agree with the authors of refs 16−19 that they are essentially due to low-coordination Co^{2+} (as proved by Drozdova et al. by EXAFS[19]) and that absorption bands characteristic of neither hydrated Co^{2+} nor $[Co^{2+}(OH)^-]^+$ species are detected after outgassing. However, the possibility of a role for Co species located at the external zeolite surface, which has not been considered in the previous UV−vis studies[16−19] or in IR studies of adsorbed probe molecules such as CO[21] and NO,[22] is very likely.

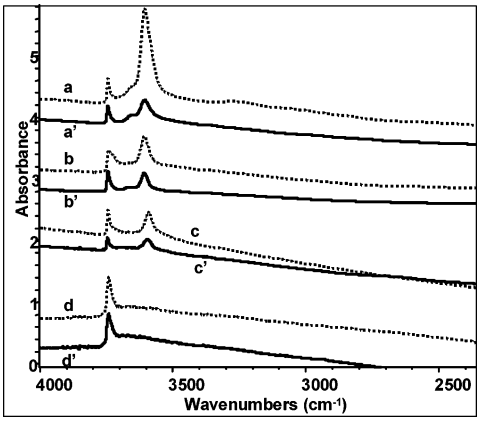

Figure 2. FT-IR spectra of samples outgassed at 773 K for 1 h: spectrum a, Co−H−FER; spectrum a′, H−FER; spectrum b, Co−H−MFI; spectrum b′, H−MFI; spectrum c, Co−H−MOR; spectrum c′, H−MOR; spectrum d, H−silica−alumina; spectrum d′, Co−H−silica−alumina.

FT-IR Studies: O−H-Stretching Bands. The IR spectra of the O−H-stretching bands of hydroxyl groups of activated Co zeolites and Co−H−silica−alumina are compared to those of the corresponding H zeolites and H−silica−alumina in Figure 2. As discussed elsewhere,[4,5] the spectra of H zeolites show a very sharp band at 3747 cm^{-1} which is due to the terminal silanol groups (located on the external surface and weakly acidic) and a broader band at 3600 cm^{-1}, due to the bridging Si−OH−Al groups that are exclusively on the inner surface and possess a strong Brønsted acidity.

The Co-exchanged samples show the same bands but with a loss of intensity. Such an intensity decrease of the O−H bands is reasonably due to the exchange of the protons by Co ions. Although a certain error (probably small) can occur in this evaluation, we can conclude that for Co−H−FER, Co−H−MFI, and Co−H−MOR, the exchange of protons, in particular of those associated with the internal bridging OHs, is evidently only partial. On the other hand, the apparent extent of exchange of such internal protons decreases with the decreasing size of the main channels (MOR > MFI > FER), and so are possibly associated with the hindered access of the Co-aquo ions into the channels during ion exchange. On the other hand, we must also mention that the terminal silanols, present on the external crystal surface, are clearly partially exchanged in a nonnegligible amount in all cases. This suggests that Co cations could also be located at the external surface.

These data can also be considered taking into account the amount of the loaded cobalt as determined by chemical analysis (Table 1). Cobalt loading is far higher for Co−H−MOR, due to its lower Si/Al atomic ratio. The analytical data showing a Co/Al atomic ratio ranging from 0.55 to 0.73 provide evidence for a partial overexchange with respect to the 0.5 value expected for the Co^{2+}/Al^{3+} atomic ratio. This can just reflect the existence of the external surface where Co can also exchange, as actually observed, with the protons of terminal silanols.

FT-IR Study of the Adsorption of Benzonitrile on Silica−Alumina and Co−Silica−Alumina. The interaction of acetonitrile with silica−alumina,[23,24] H−FER,[4,5] Co−H−FER,[14] H−MFI,[5,6] Co−H−MFI,[14] and H−MOR[7,8] has been the object of previous studies from our group.

Benzonitrile (BZN) and *o*-toluonitrile (*o*-TN), which are more hindered weakly basic molecules than acetonitrile, have been used below to discriminate between external and internal sites in the case of the zeolites.

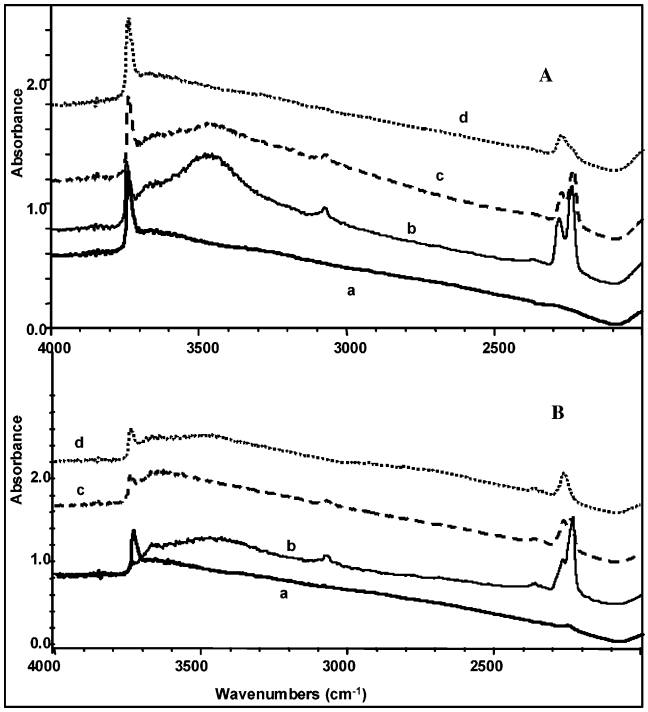

Figure 3. FT-IR spectra of (A) H−silica−alumina and (B) Co−H−silica−alumina: spectrum a, sample outgassed at 773 K for 1 h; spectrum b, sample contacted with BZN; spectrum c, sample evacuated at RT; spectrum d, sample evacuated at 523 K.

To investigate what happens on open surfaces with these molecules, we observed the interaction of BZN on silica−alumina and Co−silica−alumina (Figure 3). On silica−alumina (Figure 3A, spectra a and b) the band of terminal silanols at 3745 cm^{-1} is clearly affected by BZN adsorption, while a new band is formed near 3400 cm^{-1}. This is evidence of H-bonding of BZN on these sites. A further broad tail can be found in the region of 3400−2800 cm^{-1} similar to that observed for acetonitrile adsorption on the same solid,[25] due to a stronger interaction with the strongest terminal silanols. The CN-stretching regions for BZN adsorbed on the different Co-free solids considered here are compared in Figure 4A. On silica−alumina (Figure 4A, spectrum b) two bands are clearly observed centered at 2282 and 2239 cm^{-1} with a component at 2248 cm^{-1}. The latter band disappears when the sample is outgassed (Figure 3A, spectrum d) and also the O−H stretching at 3400 cm^{-1} disappears and the sharp band at 3745 cm^{-1} is restored.

In the CN-stretching region, liquid BZN is characterized by the CN stretching at 2229 cm^{-1} (Figure 4, spectrum a). The CN band at 2250−2230 cm^{-1} is, therefore, assigned to H-bonded BZN. The band at 2282 cm^{-1} can be assigned to BZN interacting with the Al^{3+} Lewis sites of silica−alumina, in agreement with previous studies.[25] It is well-known that when interaction with electron-withdrawing centers occurs, the CN-stretching band of nitriles shifts to higher frequencies: the stronger the interaction, the larger the shift.

Adsorption of BZN (Figure 3B, spectrum b) on Co−silica−alumina causes the perturbation of the band of terminal silanols with the parallel formation of a CN band centered at 2230 cm^{-1} (Figure 4B, spectrum b) but with components at higher frequencies. However, another band centered at 2264 cm^{-1} with a tail up to 2290 cm^{-1} is also present and persists after outgassing. This band should be assigned to BZN interacting with Lewis acid sites that are weaker than the Al^{3+} sites observed on silica−alumina. These sites are identified as Co^{2+}

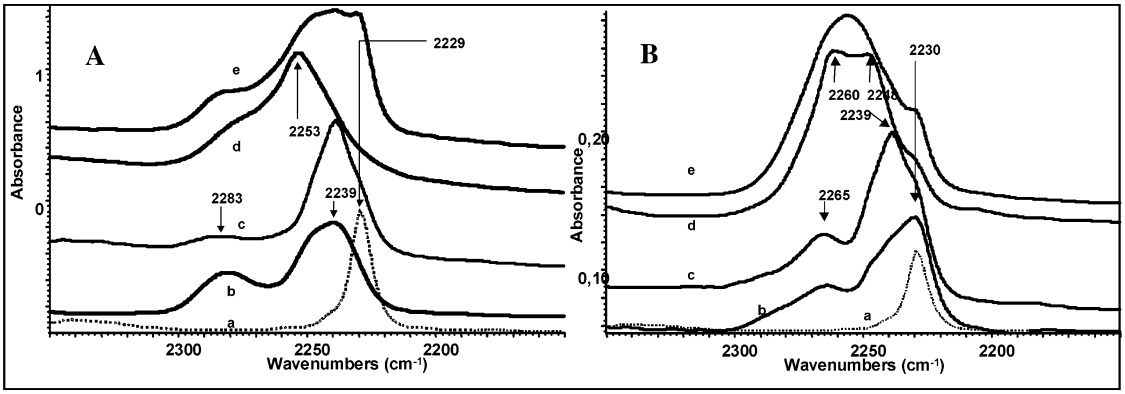

Figure 4. FT-IR spectra (CN-stretching region) of BZN interacting with (A) H samples, and (B) Co−H samples: spectrum a, liquid benzonitrile; spectrum b, benzonitrile adsorbed on silica−alumina; spectrum c, benzonitrile adsorbed on FER; spectrum d, benzonitrile adsorbed on MOR; spectrum e, benzonitrile adsorbed on MFI. In all cases there was a short outgassing at RT after adsorption on the sample activated at 773 K.

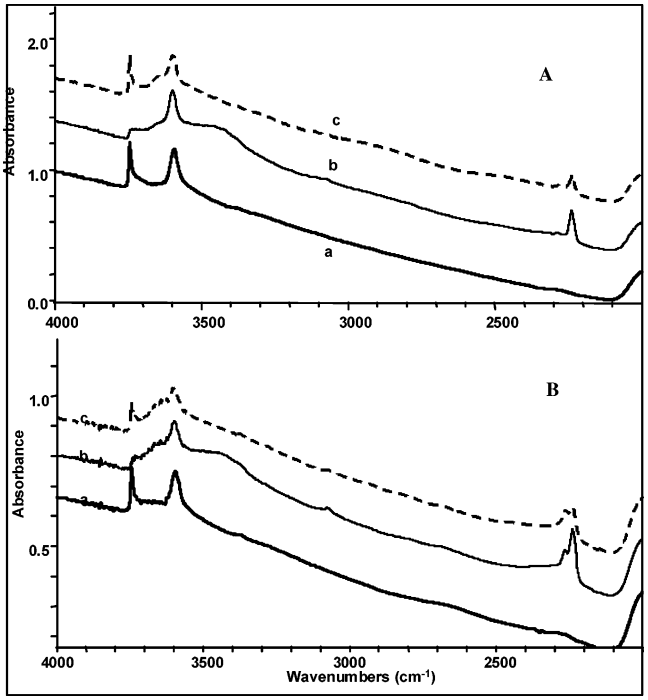

Figure 5. FT-IR spectra of (A) H−FER and (B) Co−H−FER: spectrum a, sample outgassed at 773 K for 1 h; spectrum b, sample contacted with BZN; spectrum c, sample evacuated at RT.

sites. The higher frequency components could be due to BZN interacting with Al^{3+} sites.

FT-IR Study of the Adsorption of Benzonitrile on H−FER and Co−H−FER Zeolites. The spectra recorded in the experiments of BZN adsorption onto H−FER and Co−H−FER are reported in Figure 5.

In both cases the band at 3747 cm^{-1} assigned to terminal silanol groups disappears while a new broad band is formed near 3450 cm^{-1}. The band at 3600 cm^{-1}, characteristic of the internal bridging OHs, is, on the contrary, unperturbed. The spectra also show a number of bands due to adsorbed BZN, that is, those typical of the aromatic ring at 3070 cm^{-1} (C−H stretching), 1599, 1582, 1492, and 1448 cm^{-1} (ring vibrations). BZN adsorbed on the H−FER surface shows two CN-stretching bands: one centered at 2240 cm^{-1} (but with unresolved components at both sides) and a weaker one at 2285 cm^{-1} (Figure 5A, spectra b and c and Figure 4A, spectrum c). The former band weakens upon outgassing, together with the O−H-stretching band at 3450 cm^{-1}, while the band of free silanol groups at 3747 cm^{-1} is progressively restored. On Co−H−FER in the CN-stretching region a new band at 2265 cm^{-1} (Figure 5B, spectrum c and Figure 4B, spectrum c) is visible. This feature, similar to that observed for Co−silica−alumina, arises from the interaction between BZN and cobalt sites

From these spectra we can claim that BZN perturbs only the terminal external silanol groups, whereas it cannot interact with the bridging OHs because it does not enter the cavities where they are located. This is very reasonable because of the diameters of the FER cavities (4.2 Å × 5.4 Å for the 10-ring channels along [001] and 3.5 Å × 4.8 Å for the 8-ring channels along [010])[26] and the size of the aromatic ring which has a hindrance of more than 5 Å.[27] The CN band centered at 2240 cm^{-1} is assigned to BZN interacting with silanol groups (which are known to be characterized by a quite weak acidity), whereas the 2285 cm^{-1} one is reasonably due to BZN adsorbed over Al^{3+} Lewis sites. These Lewis sites are, therefore (like terminal silanols), surely located on the external surface of H−FER. Actually, the behavior of BZN on H−FER closely parallels that of pivalonitrile (2,2-dimethylpropionitrile) previously described,[4,5] that has an even higher steric hindrance.[28]

The detection of Co−BZN complexes for Co−H−FER indicates that part of the Co ions are allocated on the external surface of the sample. These data allow us to confirm that Co exchange also occurs at the external surface so leaving cobalt ions out of the cavities. These sites act as Lewis sites.

FT-IR Study of the Adsorption of Benzonitrile on H−MFI and Co−H−MFI Zeolites. In the CN-stretching region (Figure 6A and Figure 4A, spectrum e), after adsorption of the probe molecule on the H−MFI surface, the spectra show the main maximum shifting reversibly by increasing coverage from 2240 to 2255 cm^{-1} with a sharper weak component at 2230 cm^{-1} and a shoulder at 2285 cm^{-1}. In agreement with the previously reported data for BZN adsorption over other H−MFI samples,[28] the results show that the O−H stretching of terminal silanols is shifted from 3743 to 3410 cm^{-1} upon H-bonding with BZN while the band of the bridging OHs shifts from 3608 cm^{-1} down to give the ABC spectrum at 2810, 2410, and near 1680 cm^{-1}, typical of strong quasi-symmetrical H-bonding.[29,30] The main CN-stretching maximum, shifting from 2240 to 2230 cm^{-1}, is assigned to BZN interacting with the strong Brønsted sites (bridging OHs) being in fact associated with the ABC triplet. These sites could be heterogeneous, according to the shift observed for the CN-stretching band. The sharp νCN component at 2230 cm^{-1} is due to BZN H-bonded on silanols, whereas

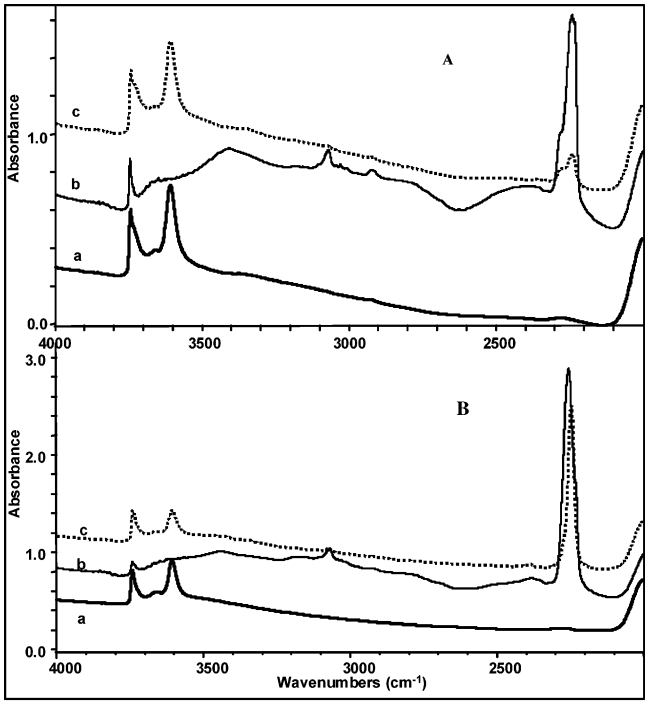

Figure 6. FT-IR spectra of (A) H−MFI and (B) Co−H−MFI: spectrum a, sample outgassed at 773 K for 1 h; spectrum b, sample contacted with BZN; spectrum c, sample evacuated at 523 K.

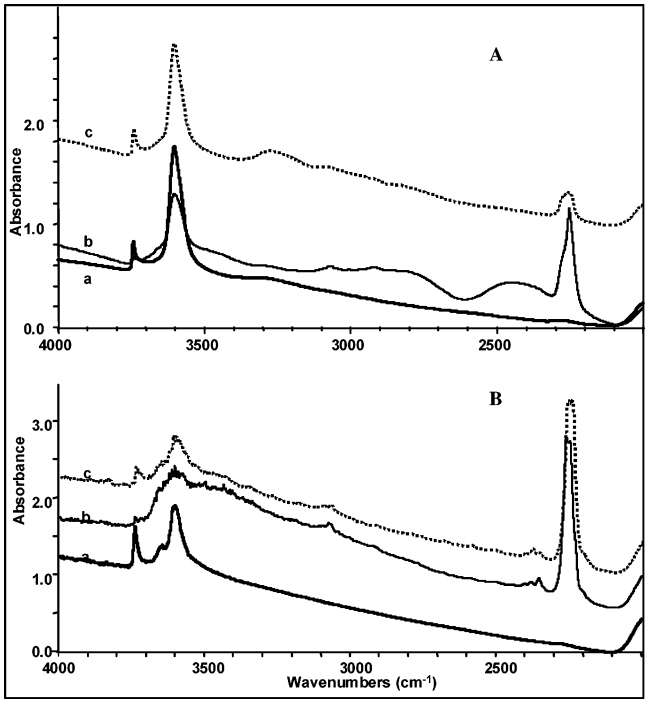

Figure 7. FT-IR spectra of (A) H−MOR and (B) Co−H−MOR: spectrum a, sample outgassed at 773 K for 1 h; spectrum b, sample contacted with BZN; spectrum c, sample evacuated at 523 K.

that at 2285 cm^{-1} is assigned to Lewis-bonded BZN. It is likely that also a small part of the 2250 cm^{-1} band is associated with a second Lewis-bonded species, being resistant to outgassing, as already reported.[5,6]

This shows that, in agreement with previous studies, BZN[28] like other monosubstituted benzenes,[31] is actually able to penetrate the cavities of MFI.

The cavities of MFI are larger than those of FER: MFI has two 10-ring intersecting channels, one 5.3 Å × 5.6 Å wide (straight, along [010]), the other 5.1 Å × 5.5 Å (sinusoidal, along [100]).[26]

The spectra of Co−H−MFI contacted with the same probe molecule are shown in Figure 6B.

In the CN-stretching region (Figure 6B and Figure 4B, spectrum e) the main, extremely strong, maximum is now observed shifting by decreasing the adsorbate partial pressure from 2250 to 2255 cm^{-1} and is not associated with the ABC triplet. It is assigned to BZN coordinated to Co Lewis sites; it resists outgassing together with the Al Lewis sites component at 2280 cm^{-1}.

It can be highlighted that the presence of Co does not cause any significant hindrance to the diffusion of BZN as the inner OHs are still entirely reachable by the probe molecule. Obviously, with the access of BZN into the MFI cavities being possible, the internal and external Co sites cannot be distinguished.

FT-IR Study of the Adsorption of Benzonitrile on H−MOR and Co−H−MOR Zeolites. The spectra of BZN adsorption onto H−MOR are reported in Figure 7A.

The spectra show that BZN perturbs a portion only of the bridging OHs (band at 3605 cm^{-1}), as previously shown for pivalonitrile (2,2-dimethylpropionitrile).[7,8]

In agreement with our previous data, we conclude that BZN interacts only with protons located toward the center of the main 12-ring channels which run along [001] and are 6.5 Å × 7.0 Å wide.[26]

The components assigned to bridging OHs lying at the intersection between main channels and the mouth of the side pockets (3609 cm^{-1}), inside the side pockets (3588 cm^{-1}), and to extraframework materials in the side pockets (3650 cm^{-1}) are unperturbed as already shown for the interaction of H−MOR with pivalonitrile.[7,8]

This is due to the lower dimension of the 8-ring compressed channels running also along [001] (2.6 Å × 5.7 Å) and of the 8-ring "side pockets" in the [010] direction (3.4 Å × 4.8 Å).[26]

The main CN-stretching component (Figure 7A and Figure 4A, spectrum e) at 2250 cm^{-1} is due to adsorption over inner Brønsted sites, whereas a weak component around 2235 cm^{-1} (observed in the subtraction spectra) corresponds to BZN over the external silanols. BZN on Lewis sites located likely at the external surface is responsible for the residual band at 2265 cm^{-1}, still present after outgassing.

In the case of Co−H−MOR BZN the band at 3605 cm^{-1}, due to the bridging OHs residual to ion exchange, retains most of its intensity upon contact with BZN and the ABC spectrum does not form. This means that these sites are not accessible to BZN, suggesting that the sites that did not undergo ion exchange are located at the mouth of the side pockets and inside the side pockets. In the CN-stretching region, a new very strong component split at 2260−2250 cm^{-1} is evident, and is assigned to BZN over Co Lewis sites.

FT-IR Studies of the Adsorption of *o*-Toluonitrile. The interaction of *o*-toluonitrile (*o*-TN), whose CN-stretching frequency is observed, in the liquid, at a slightly lower frequency than BZN (2225 vs 2229 cm^{-1}, Figure 8, spectrum a), with zeolites can give additional information on the location of the adsorption sites as the steric hindrance of *o*-TN is a little higher than that of BZN. The results concerning the interaction of *o*-TN with silica−alumina, Co−silica−alumina, H−FER, and Co−H−FER will not be discussed here because they are closely similar to those obtained with BZN. This agrees with the higher steric hindrance of *o*-TN with respect to BZN, which already does not enter the FER cavities.

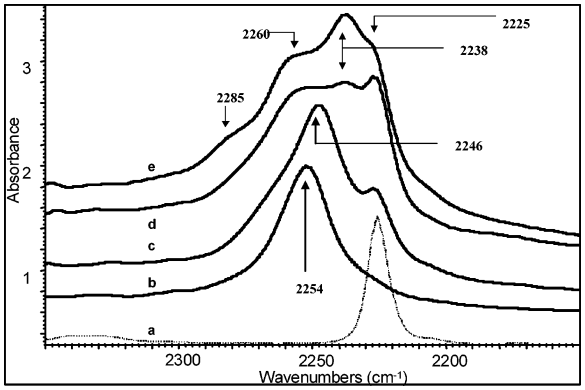

Figure 8. FT-IR spectra (CN-stretching region) of *o*-toluonitrile spectrum a, liquid *o*-toluonitrile; spectrum b, *o*-toluonitrile adsorbed on Co−H−MOR; spectrum c, *o*-toluonitrile adsorbed on H−MOR; spectrum d *o*-toluonitrile adsorbed on Co−H−MFI; spectrum e, *o*-toluonitrile adsorbed on H−MFI. In all cases there was a short outgassing at RT after adsorption on the sample activated at 773 K.

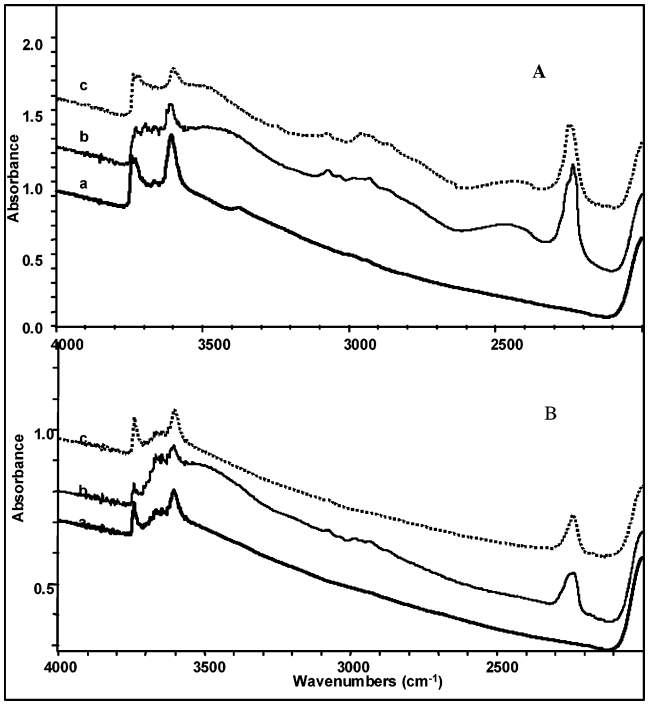

Figure 9. FT-IR spectra of (A) H−MFI and (B) Co−H−MFI: spectrum a, sample outgassed at 773 K for 1 h; spectrum b, sample contacted with *o*-TN; spectrum c, sample evacuated at 523 K.

FT-IR Studies of the Adsorption of *o*-Toluonitrile on H−MFI and Co−H−MFI Zeolites. The adsorption of *o*-TN over H−MFI modifies the spectrum of the activated sample (Figure 9A). Both the bands at 3743 and 3608 cm^{-1} decrease but do not disappear completely upon interaction with *o*-TN. The maximum of the residual band of terminal silanols is now at 3736 cm^{-1}. At the same time a broad band at 3450 cm^{-1} and a weak ABC pattern are evident. These effects tend to become more evident with increasing contact time (1−10 min). This behavior is different from that observed upon adsorption of BZN on the same zeolite. This suggests that, because of its bigger steric hindrance, *o*-TN adsorbs immediately at the external surface but enters the cavities more slowly compared to BZN, and it reaches only the most exposed inner OHs. This agrees with the behavior of *o*-xylene on ZSM5, previously discussed.[31]

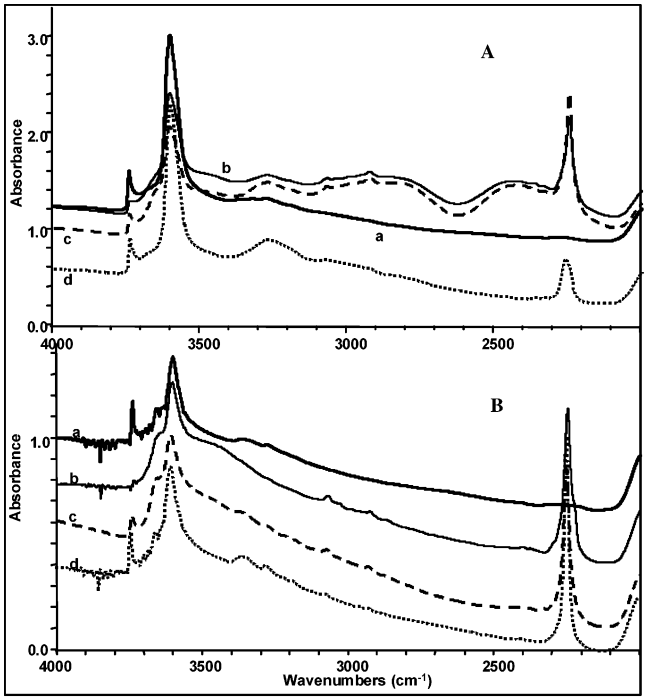

Figure 10. FT-IR spectra of (A) H−MOR and (B) Co−H−MOR: spectrum a, sample outgassed at 773 K for 1 h; spectrum b, sample contacted with *o*-TN; spectrum c, sample evacuated at RT; spectrum d, sample evacuated at 523 K.

The unperturbed terminal silanols absorbing at 3736 cm^{-1} are likely associated with extraframework species in the cavities.[9]

In the CN-stretching region the spectrum (Figure 8, spectrum b and Figure 9A) shows four components at 2230, 2240, 2258, and 2280 cm^{-1} assignable to the probe molecule adsorbed over silanols, Brønsted sites, and two Al Lewis sites, respectively. The existence of two different Lewis sites at the external surface of ZSM5 has been previously reported.[5,6]

With Co−H−MFI (Figure 9B) the band at 3608 cm^{-1} is apparently fully unaltered. Because of the ability of *o*-TN to enter (although slowly) the cavities of H−MFI, this behavior suggests that the most accessible OHs of H−MFI, likely those located near the mouth of the channels toward the external surface, are exchanged more efficiently than those located deeply inside the channels. Co exchange likely causes the obstruction of the entrance of the channels. This is in line with the size of Co^{2+} ions and its effect in narrowing the pores of zeolites. The higher frequency CN-stretching component observed for *o*-TN adsorbed on Co−H−MFI (Figures 8 and 9B) near 2260 cm^{-1} is due to *o*-TN interacting with Co ions at the external surface or at the mouth of the channels.

FT-IR Studies of the Adsorption of *o*-Toluonitrile on H−MOR and Co−H−MOR Zeolites. The spectra recorded during the experiment of adsorption of *o*-TN over H−MOR are reported in Figure 10A.

They show a situation which is closely similar to that already discussed for the interaction of BZN with H−MOR. This means that, because of the modest size difference between *o*-TN and BZN (and pivalonitrile, too), the access of *o*-TN at the MOR main channels' cavities is not significantly hindered. On the other hand, *o*-TN, like BZN, is not able to enter the compressed channels and the side pockets and is also hindered in its interaction with the sites which are at the mouth of the side pockets.

The picture relative to the interaction of *o*-TN with Co−H−MOR (Figure 10B) is also similar to that relative to the interaction of BZN with the same solid. We can note, however, that while the band of *o*-TN interacting with Co^{2+} ions here is sharp and single (2254 cm^{-1}), the corresponding band of BZN was clearly broader and split (2260, 2250 cm^{-1}). It is possible to hypothesize that BZN can enter the Co−H−MOR main channels and discriminate between internal and external Co^{2+} ions, whereas *o*-TN can only detect external Co^{2+} ions, so it cannot enter the cavity. The same occurs in the case of Co−H−MFI, where BZN enters the cavities and *o*-TN does not. If this is true, taking into account that the CN stretching of *o*-TN is located at slightly lower frequency than that of BZN, we should conclude that the external Co^{2+} ions are likely a little more polarizing than the internal ones, thus giving rise to slightly higher CN frequencies for coordinated nitriles. This agrees with the position of the CN stretching of BZN on the open surfaces of Co−silica−alumina and Co−H−FER which is at a slightly higher frequency than that of BZN adsorbed on Co−H−MFI (Figure 4B), where interaction with internal Co ions should predominate.

Conclusions

The results presented here allow us to gain information on the location and nature of Co ions in partially Co-exchanged FER, MFI, and MOR zeolites. These materials are active catalysts for the CH_4−SCR process, that is, the selective catalytic reduction of NOx by methane, as discussed elsewhere.[14]

To investigate the possible existence of Co ions at the external "open" surface of these zeolites, we also have studied Co−silica−alumina, a material which has a similar chemical composition but is an amorphous nonzeolitic solid.

The UV−vis spectra of the samples recorded after outgassing at 773 K (like for IR experiments) are closely similar to each other and to those previously reported for Co-exchanged FER, MFI, and MOR catalysts. The spectra, which all show a triplet in the region of 22 000−13 000 cm^{-1}, could be associated with low-coordination Co^{2+} ions, in agreement with previous studies.[16−19] However, their assignment to three different types of sites only located at the internal cavities (but similar for the three zeolites) that has been given by previous authors[16−19] is doubtful in our opinion, simply because the spectrum is very similar (and is a triplet) to the case of Co^{2+} ions on the open surface of Co−silica−alumina.

In the FT-IR study, the analysis of the intensity of νOH bands, which are residual in the spectra of Co-exchanged samples, indicates that both internal bridging and external terminal OHs are only partially exchanged. This is despite the theoretical slight overexchange determined by chemical analysis. In particular, it seems that, with our procedure, the extent of the exchange of the internal bridging OHs is directly dependent on the cavity size.

The use of differently hindered nitriles as basic molecular probes has been applied for the determination by FT-IR spectroscopy of the location and the acid nature of these sites.

In this paper we summarize the results obtained with benzonitrile (BZN) and *o*-toluonitrile (*o*-TN) as probes and follow previous studies where aliphatic more-or-less branched nitriles[4−8,14,28] and aromatic hydrocarbons[6,31] were applied to characterize protonic zeolites.

Both BZN and *o*-TN do not have access to the cavities of FER materials. So they are used to test the nature of the external surfaces of both H−FER and Co−H−FER. It is deduced, in agreement with previous studies,[4,5] that terminal silanols and Lewis sites are present at the external surface of H−FER, whereas the strongly Brønsted acidic bridging Si−OH−Al sites are exclusively located at the internal cavity surface of H−FER. The external surface of Co−H−FER presents, again, terminal silanols (although in smaller amounts than for H−FER due to their partial cation exchange) and Co^{2+} ions which resemble those detected also at the surface of Co−silica−alumina. Traces of Al^{3+} Lewis sites are also likely residual. The partial decrease of the band of the bridging Si−OH−Al group upon Co exchange shows that a limited exchange occurred also at the internal Brønsted sites.

BZN quickly enters into the cavities of H−MFI and gives rise to the typical strong interaction with the strong Brønsted acidic bridging Si−OH−Al sites evidenced by the so-called ABC spectrum. Additionally, it interacts with Lewis sites and, more weakly, with the external terminal silanols. Similarly, it also enters the cavities of Co−H−MFI, detecting, together with all the above sites, also medium Lewis acidic Co^{2+} ions.

o-TN, because of its higher steric hindrance, enters slowly into the cavities of H−MFI. This confirms that at the external surface (where interaction is fast) terminal silanols and Lewis sites are located. Strong Brønsted acidic bridging Si−OH−Al sites, the extent of whose perturbation increases slowly with contact time, are instead internal, like some extraframework species.

o-TN, on the contrary, does not enter the cavities of Co−H−MFI at all. In fact, in this case, the external silanol groups are perturbed whereas the residual internal bridging OHs are not. *o*-TN, on the other hand, again detects, like for Co−silica−alumina and Co−FER, medium Lewis acidic Co^{2+} ions at the external surface of Co−H−MFI.

The adsorption of *o*-TN, because of its size, therefore provides evidence for the narrowing of the channels (or of their mouth) of MFI arising from Co exchange. This also indicates that cation exchange occurs preferentially at the mouth of the channels. In fact Co−H−MFI presents a large part of bridging OHs still unexchanged but not accessible to *o*-TN.

BZN enters the main channels of H−MOR and also of Co−H−MOR (where it perturbs only the well-exposed bridging OHs), whereas it is not able to enter the compressed channels and the side pockets. This allows us to determine that the residual OHs in Co−H−MOR are inaccessible to BZN: they lie either inside or at the mouth of side pockets. This confirms that the larger the cavity, the easier the cation exchange. BZN interaction with medium Lewis acidic Co^{2+} ions is also observed, but the resulting CN band is double, suggesting that this molecule distinguishes between the Co ions at the external surface and those in the main channels.

o-TN behaves just like BZN when interacting with H−MOR. On the contrary, the CN band due to *o*-TN interacting with Co ions is sharp and single here (unlike the case of BZN) suggesting that *o*-TN only interacts with a single family of Co^{2+} ions, lying at the outer surface, and is not able (unlike BZN) to interact with Co^{2+} residing inside the main channels.

In general, these data show the existence, in all cases, of Co cations at the external surface of the exchanged zeolites and suggest that, in principle, the role of these sites in the catalytic behavior and in the optical behavior of the zeolites should not be neglected. The correlation of the obtained results suggests that the external Co^{2+} ions are a little more polarizing with respect to aromatic nitriles than the internal ones.

Acknowledgment. This work has been supported in part by CESI S. p. A. and by MIUR.

References and Notes

(1) *Zeolites for Cleaner Technologies*; Guisnet, M., Gilson, J. P., Eds.; Imperial College Press: London, 2002.
(2) Paparatto, G.; Moretti, E.; Leofanti, G.; Gatti, F. *J. Catal*. **1987**, *105*, 227.
(3) Kunieda, T.; Kim, J.-H.; Niwa, M. *J. Catal*. **1999**, *188*, 431.
(4) Trombetta, M.; Busca, G.; Lenarda, M.; Storaro, L.; Pavan M. *Appl. Catal., A* **1999**, *182*, 225.
(5) Trombetta, M.; Busca, G. *J. Catal*. **1999**, *187*, 521.
(6) Trombetta, M.; Armaroli, T.; Gutiérrez-Alejandre, A.; Ramírez, J.; Busca, G. *Appl. Catal., A* **2000**, *192*, 125.
(7) Bevilacqua, M.; Gutiérrez-Alejandre, A.; Resini, C.; Casagrande, M.; Ramírez, J.; Busca, G. *Phys. Chem. Chem. Phys.* **2002**, *4*, 4575.
(8) Bevilacqua, M.; Busca, G. *Catal. Commun.* **2002**, *3*, 497.
(9) Armaroli, T.; Bevilacqua, M.; Trombetta, M.; Milella, F.; Gutiérrez-Alejandre, A.; Ramírez, J.; Notari, B.; Willey, R. J.; Busca, G. *Appl. Catal., A* **2001**, *216*, 59.
(10) Li, W.; Yu, S. Y.; Meitzner, G. D.; Iglesia, E. *J. Phys. Chem. B* **2001**, *105*, 1176.
(11) Bulánek, R.; Novoveská, K.; Wichterlová, B. *Appl. Catal., A* **2002**, *235*, 181.
(12) Armor, J. N. *Catal. Today* **1995**, *26*, 147.
(13) Kauchy, D.; Vondrovà, A.; Dedechek, J.; Wichterlova, B. *J. Catal*. **2000**, *194*, 318.
(14) Resini, C.; Montanari, T.; Nappi, L.; Bagnasco, G.; Turco, M.; Busca, G.; Bregani, F.; Notaro M.; Rocchini, G. *J. Catal*. **2003**, *214*, 179.
(15) Campa, M. C.; De Rossi, S.; Ferraris, G.; Indovina, V. *Appl. Catal., B* **1996**, *8*, 315.
(16) Kauchy, D.; Dedechek, J.; Wichterlová, B. *Microporous Mesoporous Mater*. **1999**, *31*, 75.
(17) Dedechek, J.; Wichterlová, B. *J. Phys. Chem. B* **1999**, *103*, 1462.
(18) Dedechek, J.; Kauchy, D.; Wichterlová, B. *Microporous Mesoporous Mater*. **2000**, *35*−*36*, 483.
(19) Drozdova, L.; Prins, R.; Dedechek, J.; Sobalik, Z.; Wichterlová, B. *J. Phys. Chem. B* **2002**, *106* 2240.
(20) Yan, J.-Y.; Kung, H. H.; Schtler, W. M. H.; Kung, M. C. *J. Catal*. **1998**, *175*, 294.
(21) Hadjiivanov, K.; Tsyntsarski, B.; Venkov, Tz.; Daturi, M.; Saussey J.; Lavalley, J.-C. *Phys. Chem. Chem. Phys.* **2003**, *5*, 243.
(22) Ivanova, E.; Hadjiivanov, K.; Klissurski, D.; Bevilacqua, M.; Armaroli T.; Busca, G. *Microporous Mesoporous Mater*. **2001,** *46*, 299.
(23) Scokart, P. O.; Rouxhet, P. G. *J. Colloid Interface Sci.* **1982**, *80*, 96.
(24) Trombetta, M.; Busca, G.; Rossini, S.; Piccoli, V.; Cornaro, U.; Guercio, A.; Catani, R.; Willey, R. J. *J. Catal.* **1998**, *179*, 581.
(25) Zecchina, A.; Bordiga, S.; Spoto, G.; Marchese, L.; Petrini, G.; Leofanti G.; Padovan, M.; *J. Phys. Chem*. **1992**, *96*, 499.
(26) International Zeolite Association, Database of Zeolite Structures. http://www.zeolites.ethz.ch/Zeolites/StdAtlas.htm (accessed March 2003).
(27) Satterfield, C. N. *Heterogeneous Catalysis in Practice*, 2nd ed.; McGraw-Hill: New York, 1990; p 239.
(28) Armaroli, T.; Gutiérrez Alejandre, A.; Bevilacqua, M.; Trombetta, M.; Milella, F.; Ramírez J.; Busca, G. In *Zeolites and Mesoporous Materials at the Dawn of the 21st Century*; Galarneau, A., Di Renzo, F., Fajula F., Vedrine, J., Eds.; Studies in Surface Science and Catalysis [electronic edition]; Elsevier: Amsterdam, 2001; *135*, 13P25.
(29) Pelmenschikov, A. G.; vanSanten, R. A. *J. Phys. Chem.* **1993**, *97***,** 10678.
(30) Zecchina, A.; Bordiga, S.; Spoto, G.; Scarano, D.; Spanò G.; Geobaldo, F. *J. Chem. Soc., Faraday Trans.* **1996**, *92*, 4863.
(31) Armaroli, T.; Bevilacqua, M.; Trombetta, M.; Gutiérrez Alejandre, A.; Ramìrez, J.; Busca, G. *Appl. Catal., A* **2001**, *220*, 181.